

**Percolation on an isotropically directed lattice**Aurelio W. T. de Noronha,<sup>1</sup> André A. Moreira,<sup>1</sup> André P. Vieira,<sup>2,3</sup> Hans J. Herrmann,<sup>1,3</sup>  
José S. Andrade Jr.,<sup>1</sup> and Humberto A. Carmona<sup>1</sup><sup>1</sup>*Departamento de Física, Universidade Federal do Ceará, 60451-970 Fortaleza, Ceará, Brazil*<sup>2</sup>*Instituto de Física, Universidade de São Paulo, Caixa Postal 66318, 05314-970 São Paulo, Brazil*<sup>3</sup>*Computational Physics for Engineering Materials, IfB, ETH Zurich, Schafmattstrasse 6, CH-8093 Zürich, Switzerland*

(Received 8 August 2018; published 11 December 2018)

We investigate percolation on a randomly directed lattice, an intermediate between standard percolation and directed percolation, focusing on the isotropic case in which bonds on opposite directions occur with the same probability. We derive exact results for the percolation threshold on planar lattices, and we present a conjecture for the value of the percolation-threshold in any lattice. We also identify presumably universal critical exponents, including a fractal dimension, associated with the strongly connected components both for planar and cubic lattices. These critical exponents are different from those associated either with standard percolation or with directed percolation.

DOI: [10.1103/PhysRevE.98.062116](https://doi.org/10.1103/PhysRevE.98.062116)**I. INTRODUCTION**

In a seminal paper published some 60 years ago, Broadbent and Hammersley [1] introduced the percolation model, in a very general fashion, as consisting of a number of sites interconnected by one or two directed bonds that could transmit information in opposite directions. However, over the years most of the attention has been focused on the limiting cases of standard percolation, in which bonds in both directions are either present or absent simultaneously, and of directed percolation, in which only bonds in a preferred direction are allowed. While standard percolation represents one of the simplest models for investigating critical phenomena in equilibrium statistical physics [2], directed percolation has become a paradigmatic model for investigating nonequilibrium phase transitions [3]. Moreover, it has been shown that the isotropic case, in which bonds in both opposite directions are present with the same probability, is a very particular case, with any amount of anisotropy driving the system into the same universality class as that of directed percolation [10,13,33].

The case of percolation on isotropically directed lattices has received much less attention. This modified percolation model should be particularly relevant to the understanding of a large number of physical systems. For instance, in the same way that standard percolation was shown to be related to other models in statistical mechanics [4], one could expect percolation on isotropically directed lattices to be related to statistical systems with nonsymmetric interactions [5]. It has been shown that identifying the connected component systems with nonsymmetric interactions can elucidate questions regarding the controllability [6] and observability [7] of these systems. Percolation with directed bonds has also been investigated in the field of traffic dynamics [8]. Redner [9–11] formulated the problem of percolation on isotropically directed lattices as a random insulator-resistor-diode circuit model, in which single directed bonds represent diodes, allowing current to flow in

only one direction, while double bonds in opposite directions represent resistors and absent bonds represent insulators.

Focusing on hypercubic lattices, he employed an approximate real-space renormalization-group treatment that produces fixed points associated with both standard percolation (in which only resistors and insulators are allowed) and directed percolation (in which only insulators and diodes conducting in a single allowed direction are present), as well as other “mixed” fixed points controlling lines of critical points, for cases in which all three types of circuit elements are present. The crossover from isotropic to directed percolation when there is a slight preference for one direction was studied via computer simulations [12] and renormalized field theory [13,14]. More recently, the same crossover problem was independently investigated on the square and on the simple-cubic lattices by Zhou *et al.* [15], who dubbed their model “biased directed percolation.”

We are interested here in percolation of isotropically directed bonds in which bonds in opposite directions are present with the same probability, possibly along with vacancies and undirected bonds. It has been conjectured that this model is in the same universality class as standard percolation [13,15], however these works have focused on the sets of nodes that can be reached from a given point. In fact, when considering directed bonds, it is possible that site A can be reached from site B, while site B cannot be reached from site A, which therefore calls for a redefinition of a cluster. Percolation of directed bonds was investigated within the context of complex networks [8,16–22], where the concept of strongly connected components (SCCs) has been adopted [23], defined as those sets of points that can be mutually reached following strictly the bond directions. A critical state of the model can be characterized as the point where a giant strongly connected component (GSCC) is formed [16]. Alternatively, one can define a giant cluster formed by all the sites that can be reached from a given site following bond directions (GOUT) [16], and determine the critical point where such a cluster is

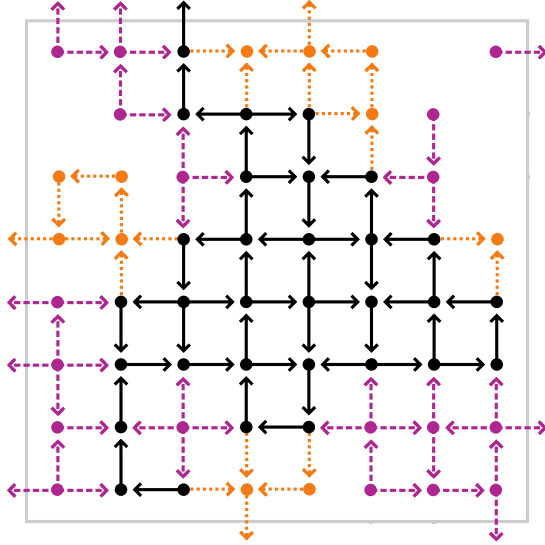


FIG. 1. A square lattice where each pair of nearest neighbors is connected by a directed bond at the critical point [15]. The color code is as follows: Black continuous lines indicates nodes and bonds comprising the largest strongly connected component (GSCC), that is, the largest set of nodes that can be mutually reached from each other. Dotted orange lines indicates nodes and bonds outside the GSCC that can be reached from nodes in the GSCC. Dashed purple lines indicates nodes and bonds outside the GSCC from where nodes in the GSCC can be reached. The largest outgoing (incoming) component [GOUT (GIN)] includes all nodes of the GSCC augmented by the orange (purple) nodes, respectively. Light grey indicates nodes and bonds outside both GIN and GOUT. Bonds exiting the enclosing box represent connections through the periodic boundary condition.

formed. Alternatively, one can define a giant cluster formed by all the sites that can be reached from a given site following bond directions [16], and determine the critical point where such a cluster is formed. There is no logical need for these two points to be the same, leaving the possibility of two distinct phase transitions existing in this model [17]. However, both for regular lattices, as we will show here, and for some complex networks [16], these two objects form at the same critical point. In Fig. 1 we show an example of a square lattice at the critical point.

This paper is organized as follows. In Sec. II we define the model and present calculations of percolation thresholds. In Sec. III we discuss some exact results on a hierarchical lattice that shed light on the critical state of this model. Our computer simulation results are presented in Sec. IV, while Sec. V is dedicated to a concluding discussion.

## II. DEFINITION OF THE MODEL AND CALCULATION OF PERCOLATION THRESHOLDS

We work on  $d$ -dimensional regular lattices. All sites are assumed to be present, but there are a few possibilities for the connectivity between nearest neighbors. With probability  $p_0$  they may not be connected (indicating a vacancy). With probability  $p_1$  they may be connected by a directed bond (with equal probabilities for either direction). Finally, with probability  $p_2$  neighbors may be connected by an undirected

bond (or equivalently by two having opposite directions). Of course, we must fulfill  $p_0 + p_1 + p_2 = 1$ .

A simple heuristic argument yields an expression for the critical threshold for percolation of isotropically directed bonds. Starting from a given site  $i$  on a very large lattice, the probability  $p_{nn}$  that a particular nearest-neighbor site can be reached from  $i$  is given by the probability that both directed bonds are present between these neighbors ( $p_2$ ) plus the probability that there is only one directed bond and that it is oriented in the appropriate direction ( $\frac{1}{2}p_1$ ). As the distribution of orientations is on average isotropic, the critical threshold must depend only on  $p_{nn}$ . In fact, using the Leath-Alexandrowicz method [24,25], it can be shown [15] that the clusters of sites reached from a seed site in percolation of directed bonds with a given  $p_{nn}$  are identically distributed to the clusters of standard percolation with an occupation  $p_{sp}$ , as long as  $p_{sp} = p_{nn}$ . Therefore, we conclude that the critical percolation probabilities of our model should fulfill

$$p_2 + \frac{1}{2}p_1 = p_c, \quad (1)$$

in which  $p_c$  is the bond-percolation threshold for standard percolation in the lattice.

We can use duality arguments to show that Eq. (1) is indeed exact for the square, triangular, and honeycomb lattices. A duality transformation for percolation of directed bonds on planar lattices was previously introduced [10] to derive the percolation threshold on the square lattice. The transformation states that every time a directed bond is present in the original lattice, the directed bond in the dual lattice that crosses the original bond forming an angle of  $\frac{\pi}{2}$  clockwise will be absent. With the opposite also holding, namely every time a directed bond is absent in the original lattice, in the dual lattice the bond forming an angle  $\frac{\pi}{2}$  clockwise will be present. Of course, an undirected bond (or alternatively two bonds in opposite directions) in the original lattice corresponds to a vacancy in the dual lattice, and vice versa. Figure 2(a) shows a configuration of percolation of directed bonds on the triangular lattice and the corresponding dual honeycomb lattice.

Denoting by  $q_0$ ,  $q_1$ , and  $q_2$  the respective probabilities that there is a vacancy, a single directed bond, or an undirected bond between nearest neighbors on the dual lattice, the transformation allows us to write

$$q_0 = p_2, \quad q_1 = p_1, \quad q_2 = p_0. \quad (2)$$

From these results and the normalization conditions

$$p_0 + p_1 + p_2 = q_0 + q_1 + q_2 = 1, \quad (3)$$

we immediately obtain

$$\frac{1}{2}(p_2 + q_2) + \frac{1}{2}p_1 = \frac{1}{2},$$

which is valid for any choice of the probabilities. As already noticed by Redner [10], for the square lattice, which is its own dual, we must have  $p_2 = q_2$  at the percolation threshold, yielding

$$p_2 + \frac{1}{2}p_1 = \frac{1}{2}, \quad (4)$$

in agreement with Eq. (1). Here, of course, we assume that there is only one critical point.

The triangular and the honeycomb lattices are related by the duality transformation, as illustrated in Fig. 2(a), and

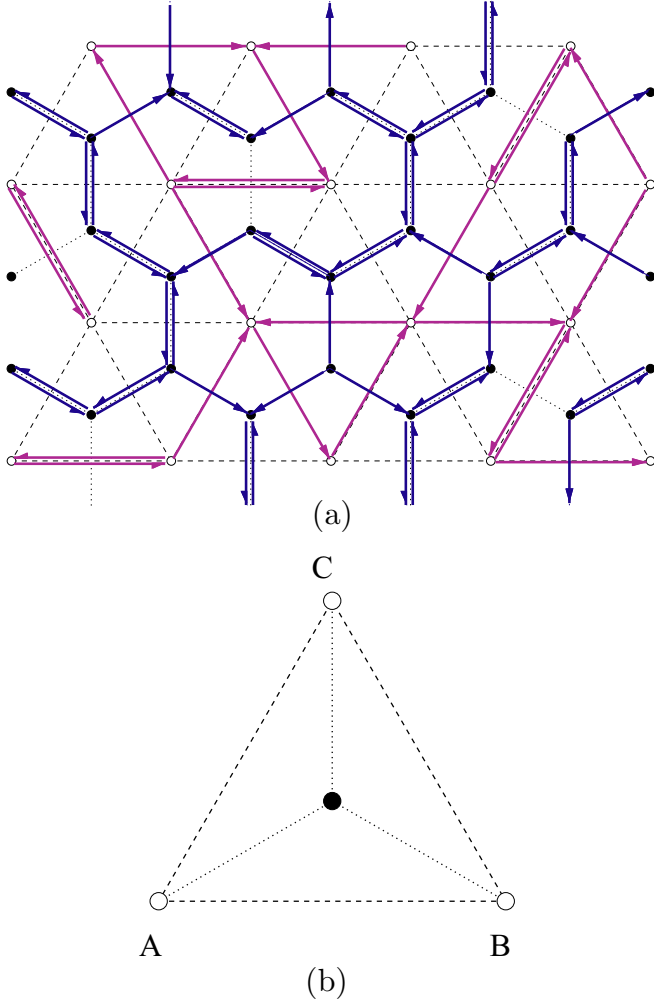


FIG. 2. (a) Illustration of a configuration of percolation of directed bonds on the triangular (white sites, lighter purple arrows) and honeycomb (black sites, darker blue arrows) lattices, related by the dual transformation defined in the text. (b) The sites involved in the star-triangle transformation discussed in the text.

we now use a star-triangle transformation [27] to calculate their bond-percolation thresholds. Based on enumerating the configurations of bonds connecting the sites identified in Fig. 2(b), we can calculate the probabilities  $P$  and  $Q$  of connections between the sites on the star and on the triangle, respectively. For the probability that site A is connected only to site B or only to site C, we obtain

$$P_{AB} = \frac{1}{2}p_1p_2^2 + \frac{1}{2}p_1^2p_2 + \frac{1}{8}p_1^3 + p_0p_2^2 + p_0p_1p_2 + \frac{1}{4}p_0p_1^2,$$

$$Q_{AB} = \frac{1}{4}q_1^2q_2 + \frac{1}{8}q_1^3 + q_0q_1q_2 + \frac{1}{2}q_0q_1^2 + q_0^2q_2 + \frac{1}{2}q_0^2q_1,$$

with  $P_{AC} = P_{AB}$  and  $Q_{AC} = Q_{AB}$ . For the probability that site A is connected to both sites B and C, we have

$$P_{ABC} = p_2^3 + \frac{3}{2}p_1p_2^2 + \frac{3}{4}p_1^2p_2 + \frac{1}{8}p_1^3,$$

$$Q_{ABC} = q_2^3 + 3q_1q_2^2 + \frac{9}{4}q_1^2q_2 + \frac{1}{2}q_1^3 + 3q_0q_2^2 + 3q_0q_1q_2 + \frac{3}{4}q_0q_1^2.$$

At the percolation threshold, we must have  $P_{AB} = Q_{AB}$  and  $P_{ABC} = Q_{ABC}$ , and taking into account the normalization conditions in Eq. (3), we obtain

$$p_2 + \frac{1}{2}p_1 = 1 - 2 \sin \frac{\pi}{18} = p_c^{(\text{honeycomb})} \quad (5)$$

and

$$q_2 + \frac{1}{2}q_1 = 2 \sin \frac{\pi}{18} = p_c^{(\text{triangular})}, \quad (6)$$

again in agreement with Eq. (1).

All these predictions show that at least one of the critical percolation points of isotropically directed bonds, when a giant out-going component (GOUT) is formed, can be simply related to the model of standard percolation by Eq. (1). Our numerical results indicate that the critical point defined by the formation of a GSCC coincides with the formation of a GOUT. However, as we show in the following section, compared to the GOUT, the GSCC has a different set of critical exponents.

### III. CRITICAL STATE OF THE PERCOLATION OF ISOTROPICALLY DIRECTED BONDS

Redner [9,10] and Dorogovtsev [26] solved exactly percolation of directed bonds on a hierarchical lattice obtained by iterating the process shown in Fig. 3. Having the probabilities  $p_0$ ,  $p_1$ , and  $p_2$  at a given generation of the process, renormalization-group calculations allow one to determine the probabilities  $p'_0$ ,  $p'_1$ , and  $p'_2$  of the next generation. The scale-invariant states are the fixed points of the renormalization

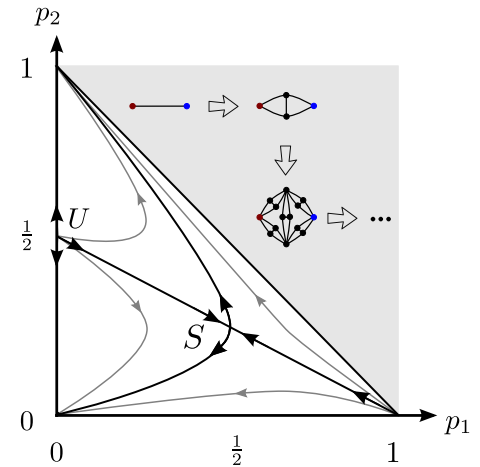


FIG. 3. Phase diagram for percolation of isotropically directed bonds on the hierarchical lattice obtained as the limit of the process displayed. Redner [9,10] and Dorogovtsev [26] used the renormalization group to solve exactly this model on the shown hierarchical lattice. The directions of the lines indicate the renormalization-group flux. The critical line  $p_2 + p_1/2 = 1/2$  coincides with the critical line for percolation of isotropically directed bonds on the square lattice. The renormalization group shows that any point on the critical line, besides  $U = (0, 1/2)$ , which corresponds to the critical point of standard percolation, will display the same scale-invariant behavior as a point  $S$  located along the critical line, suggesting the possibility that percolation of isotropically directed bonds may be in a different universality class from standard percolation.

group. As shown in Fig. 3, two of those points represent the trivial cases of a fully disconnected lattice  $p_0 = 1$  and a fully connected lattice  $p_2 = 1$ . Another fixed point is  $p_1 = 0$ , with  $p_2 = 1/2$  representing the critical scale-invariant state for standard percolation in this hierarchical lattice, while the remaining one,  $p_1 = 0.49142$  with  $p_2 = 0.25429$ , is the critical scale-invariant state for percolation of isotropically directed bonds in this hierarchical lattice. Surprisingly, this hierarchical lattice has similarities with the square lattice [9,10], as it can predict exactly not only the critical point of standard percolation, but also the whole critical line  $p_2 + p_1/2 = 1/2$ . With the exception of the critical state of standard percolation, all the other points along the critical line converge through the renormalization process toward the scale-invariant state of percolation of isotropically directed bonds.

Although these renormalization-group calculations do not yield precise predictions for the correlation-length exponent  $\nu$  in two dimensions, they give the same value  $\nu = \ln_2(13/8) \approx 1.428$  for both standard percolation as well as percolation of isotropically directed bonds [9,10]. Moreover, there are two order-parameter exponents  $\beta_1 = 0.1342$  and  $\beta_2 = 0.1550$  that are related to clusters that percolate in a single direction or in both directions, respectively [9,10]. Again here the method does not obtain exactly the value of the exponent  $\beta$  for two dimensions, presented in the next section, but it shows that  $\beta_1$  is the same value as the one obtained for standard percolation in this hierarchical lattice, while  $\beta_2$  is shown to be a different exponent. These two different exponents indicate, at least for this hierarchical lattice, that percolation on isotropically directed bonds is tricritical.

In the next section, we show that simulation results for the square, honeycomb, and triangular lattices confirm Eqs. (4)–(6). Furthermore, we show that indeed the fractal dimensions of the two forms of critical giant clusters, GSCC and GOUT, are different from each other, but seemingly universal among the different lattices.

**IV. SIMULATION RESULTS**

We start by describing our results for two dimensions, while the 3D case will be discussed subsequently. We sim-

ulated bidimensional lattices with linear size ranging from  $L = 32$  to 8192, taking averages over a number of samples ranging from 38 400 (for  $L = 32$ ) to 150 (for  $L = 8192$ ), halving the number of samples each time that the linear size was doubled. Periodic boundary conditions were employed.

Besides checking the predictions for the percolation threshold, our goal is to obtain the values of the critical exponents associated with (i) clusters that can be traversed in one direction and (ii) clusters that can be traversed in both directions. In the language of complex networks, these clusters correspond in case (i) to giant out-components (GOUT) and in case (ii) to the giant strongly connected component (GSCC). For each sample, we identified all the SCCs by using Tarjan’s algorithm [23], and we calculated their size distribution. At the percolation threshold, we also looked at the GOUT, which corresponds to the GSCC augmented by sites outside of it that can be reached from those in the GSCC. By symmetry, the statistical properties of the GOUT must be the same as those of the giant in-component (GIN), defined as the set of sites not in the GSCC from which we can reach the GSCC, augmented by sites in the GSCC itself. Figure 1 shows an example of a square lattice with  $L = 16$ , indicating the GSCC, the GOUT, and the GIN. Some of the results presented next were obtained with the help of the GRAPH TOOL software library [28].

We define the order parameter here as the fraction of sites belonging to the largest SCC. For an infinite planar lattice, this order parameter should behave as

$$\lim_{L \rightarrow \infty} \frac{\langle S \rangle}{L^2} \sim (p - p_c)^{\beta_{\text{sc}}}, \tag{7}$$

where  $\langle S \rangle$  is the average size of the largest SCC,  $p$  is a parameter that controls the distance to the critical point  $p_c$ , and  $\beta_{\text{sc}}$  is expected to be a universal critical exponent. A finite-size scaling ansatz for the order parameter is

$$\frac{\langle S \rangle}{L^2} \sim L^{-\beta_{\text{sc}}/\nu} f_1((p - p_c)L^{1/\nu}), \tag{8}$$

in which  $\nu$  is the correlation-length critical exponent and  $f_1(x)$  is a scaling function. From this ansatz, we see that

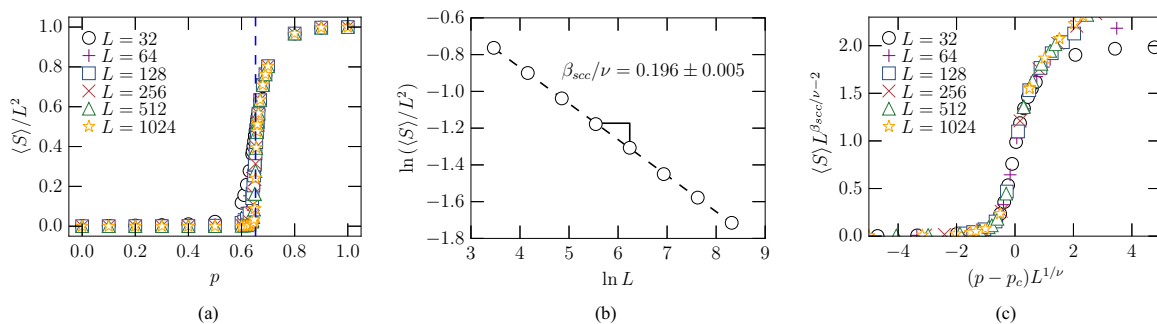


FIG. 4. These results correspond to a honeycomb lattice where each possible directed bond is occupied with probability  $p$ , with opposite bonds between the same pair of sites being present with probability  $p^2$ , as parametrized in Eq. (13). (a) The order parameter for percolation of isotropically directed bonds defined as the fraction of nodes in the largest strongly connected component (GSCC). (b) At the critical point, the fraction occupied by the GSCC decays as a power law, yielding the exponent  $\beta_{\text{sc}}/\nu$ . (c) Using the value obtained for  $\beta_{\text{sc}}/\nu$ , and assuming that the exponent  $\nu$  for percolation of isotropically directed bonds is the same as in standard percolation,  $\nu = 4/3$ , we can collapse all the curves near the critical point. Here, and in all other plots, error bars are smaller than the symbols.

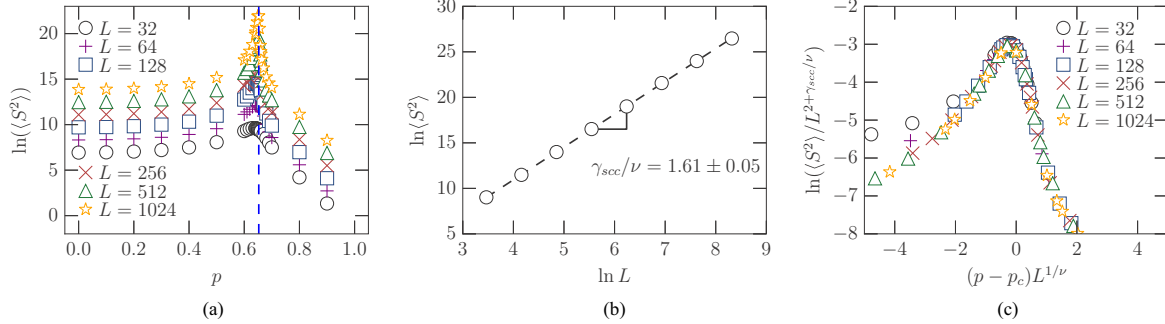


FIG. 5. These results correspond to a honeycomb lattice where each possible directed bond is occupied with probability  $p$ , with opposite bonds between the same pair of sites being present with probability  $p^2$ , as parametrized in Eq. (13). (a) The second moment of the distribution of sizes of SCCs, excluding the largest SCC. (b) At the critical point, the second moment grows as a power law, yielding the exponent  $\gamma_{\text{scc}}/\nu$ . (c) Using the value obtained for  $\gamma_{\text{scc}}/\nu$ , and assuming  $\nu = 4/3$ , we can collapse all the curves near the critical point.

precisely at the critical point we should have

$$\frac{\langle S \rangle}{L^2} \sim L^{-\beta_{\text{scc}}/\nu}. \tag{9}$$

Similarly, we can look at the second moment of the SCC size distribution (excluding the GSCC), which, for an infinite lattice, should behave as

$$\lim_{L \rightarrow \infty} \langle S^2 \rangle \sim (p - p_c)^{-\gamma_{\text{scc}}}, \tag{10}$$

with  $\gamma_{\text{scc}}$  being another universal critical exponent. The corresponding finite-size scaling ansatz is

$$\langle S^2 \rangle \sim L^{\gamma_{\text{scc}}/\nu} f_2((p - p_c)L^{1/\nu}), \tag{11}$$

where  $f_2(x)$  is also a scaling function, and precisely at the critical point we should have

$$\langle S^2 \rangle \sim L^{\gamma_{\text{scc}}/\nu}. \tag{12}$$

To obtain values for these critical exponents, we have to introduce a parametrization of the probabilities  $p_0$ ,  $p_1$ , and  $p_2$ . We performed two different sets of simulations, with different parametrizations. In the first set of numerical experiments, bonds were occupied with probabilities parametrized as

$$p_0 = (1 - p)^2, \quad p_1 = 2p(1 - p), \quad p_2 = p^2, \tag{13}$$

with  $0 \leq p \leq 1$ , so that, according to Eq. (1), we have  $p = p_c$  at the percolation threshold. This corresponds to randomly assigning one directed bond with probability  $p$  on each possible direction of each pair of nearest neighbors; two opposite directed bonds between the same pair correspond to an undirected bond.

Figure 4 shows results for the SCC order parameter for honeycomb lattices with sizes ranging from  $L = 32$  to 1024. As depicted in Fig. 4(a), the threshold probability is consistent with the result  $p \simeq 0.653$  predicted by Eq. (5). Figure 4(b) plots the SCC order parameter at the critical point, which is expected to scale as in Eq. (9), a scaling form from which we extract  $\beta_{\text{scc}}/\nu = 0.196 \pm 0.005$ . Finally, Fig. 4(c) shows a rescaling of the finite-size results according to Eq. (8). It is a well known fact [29] that percolation has a single length scale given by the correlation length  $\xi$  that diverges at the critical point as  $\xi \sim N^{-\nu}$ . Since there is no reason to expect that percolation on isotropically directed lattices introduces other

length scales, it is reasonable to assume that the exponent  $\nu$  controlling the scale divergence of SCCs near the critical point is the same as in traditional percolation. This conjecture is supported by the renormalization-group predictions of Redner [9] and of Janssen and Stenull [13,15] for the square lattice. Therefore, the best data collapse is obtained assuming for the correlation-length critical exponent the same value as in standard percolation,  $\nu = \frac{4}{3}$ , which leads to

$$\beta_{\text{scc}} = 0.264 \pm 0.008.$$

For the second moment of the SCC size distribution, Fig. 5 shows results for honeycomb lattices. As shown in Fig. 5(a), the value of the percolation threshold is compatible with the prediction of Eq. (5), while from Fig. 5(b) and Eq. (12) we obtain  $\gamma_{\text{scc}}/\nu = 1.61 \pm 0.05$ . Again, the best data collapse of Eq. (11), shown in Fig. 5(c), is obtained by using  $\nu = \frac{4}{3}$ , yielding

$$\gamma_{\text{scc}} = 2.15 \pm 0.07.$$

Table I summarizes the critical exponents obtained under the first parametrization for the triangular, square, and honeycomb lattices. We mention that the values obtained for  $\beta_{\text{scc}}$  and  $\gamma_{\text{scc}}$  are all compatible with values extracted from the simulation results by fitting the data for the largest linear size with the scaling predictions in Eqs. (7) and (10). We also measured the mass of the GSCC, denoted by  $M_{\text{scc}}$ , which is predicted to follow

$$M_{\text{scc}} \sim L^{d_{\text{scc}}},$$

TABLE I. Values of the critical exponents related to the SCCs, as obtained for the triangular, square, and hexagonal lattices, for the cases in which each possible directed bond is occupied with probability  $p$ , with opposite bonds between the same pair of sites being present with probability  $p^2$ , as parametrized in Eq. (13). Numbers in parentheses indicate the estimated error in the last digit.

Lattice	$\beta_{\text{scc}}$	$\gamma_{\text{scc}}$	$d_{\text{scc}}$
Triangular	0.264(8)	2.15(7)	1.804(5)
Square	0.261(5)	2.13(3)	1.801(8)
Hexagonal	0.27(1)	2.15(7)	1.80(1)

TABLE II. Values of the critical exponents related to the SCCs, as obtained for the triangular, square, and hexagonal lattices for the case in which undirected bonds appear only when all possible vacancies have already been occupied by a directed bond, as parametrized by Eq. (14). Numbers in parentheses again indicate the estimated error in the last digit. Within the error bars, these values are compatible with those of Table I.

Lattice	$\beta_{\text{sc}}c$	$\gamma_{\text{sc}}c$	$d_{\text{sc}}c$	$\tau_{\text{sc}}c$
Triangular	0.26(1)	2.16(8)	1.805(8)	2.07(9)
Square	0.26(1)	2.17(4)	1.802(8)	2.11(8)
Hexagonal	0.27(1)	2.16(7)	1.80(1)	2.12(8)

with a fractal dimension

$$d_{\text{sc}}c = 2 - \beta_{\text{sc}}c/\nu.$$

This is confirmed by the measurements of  $d_{\text{sc}}c$  reported in the last column of Table I.

In the second set of simulations, bonds were occupied with probabilities

$$\begin{aligned} p_0 &= \max(0, 1 - 2p), & p_1 &= 2 \min(p, 1 - p), \\ p_2 &= \max(0, 2p - 1), \end{aligned} \tag{14}$$

again with  $0 \leq p \leq 1$ . These probabilities mean that for  $p \leq \frac{1}{2}$  there are no undirected bonds, while for  $p \geq \frac{1}{2}$  there are no vacancies. Exactly at  $p = \frac{1}{2}$  there is a randomly directed bond between each pair of nearest neighbors. Again, according to Eq. (1), we have  $p = p_c$  at the percolation threshold. The results for the GSCC properties measured under this second parametrization are compatible with those obtained under the first parametrization. As shown in Table II, the critical exponents  $\beta_{\text{sc}}c$  and  $\gamma_{\text{sc}}c$  and the fractal dimension  $d_{\text{sc}}c$  are all compatible with the values obtained under the first parametrization.

Under the second parametrization, besides measuring the mass of the GSCC associated with the fractal dimension  $d_{\text{sc}}c$ , we also measured the mass of the GOUT, denoted by  $M_{\text{out}}$ ,

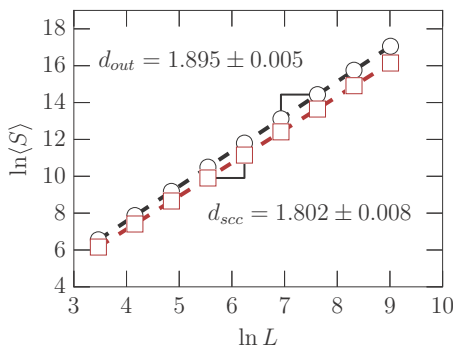


FIG. 6. The fractal dimensions for the GSCC (squares) and the GOUT (circles). These results concern square lattices where all nearest neighbors are connected by a directed bond. This corresponds to the critical condition when using the parametrization given by Eq. (14). While the fractal dimension of GOUT is compatible with that of standard percolation clusters, the GSCCs have a smaller fractal dimension.

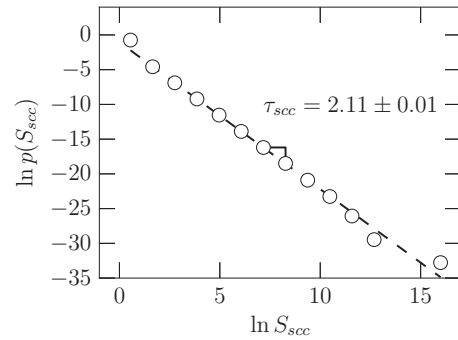


FIG. 7. Scaling behavior of the SCC size distribution  $p(S)$  for a square lattice with  $L = 8196$ , under the second parametrization.

which scales as

$$M_{\text{out}} \sim L^{d_{\text{out}}},$$

where  $d_{\text{out}}$  is a fractal dimension. We expect  $d_{\text{sc}}c \leq d_{\text{out}}$ , as the GSCC is a subset of the GOUT. Indeed, as shown in Fig. 6, for the square lattice at the critical point, the fractal dimension  $d_{\text{out}}$  of the GOUT is compatible with the exact fractal dimension  $d_f = 91/48$  [29] of the critical percolating cluster in standard percolation, while the value for  $d_{\text{sc}}c$  is about 10% smaller.

Finally, we looked at the exponents  $\tau_{\text{sc}}c$  and  $\sigma_{\text{sc}}c$  associated with the SCC size distribution, expected to scale as

$$p(S) \sim S^{-\tau_{\text{sc}}c} f_3[(p - p_c)S^{\sigma_{\text{sc}}c}], \tag{15}$$

where  $f_3(x)$  is yet another scaling function. The Fisher exponent  $\tau_{\text{sc}}c$  associated with the scaling behavior of the SCC size distribution  $p(S)$  at the critical point is defined as

$$p(S) \sim S^{-\tau_{\text{sc}}c}.$$

Figure 7 shows  $p(S)$  as a function of  $S$  for a square lattice with linear size  $L = 8196$  at the percolation threshold. The value  $\tau_{\text{sc}}c = 2.11 \pm 0.08$  obtained is compatible with the scaling relation  $\tau_{\text{sc}}c = 2 + \beta_{\text{sc}}c/(\beta_{\text{sc}}c + \gamma_{\text{sc}}c)$ . Values of  $\tau_{\text{sc}}c$  for the three lattices are reported in the last column of Table II. On the

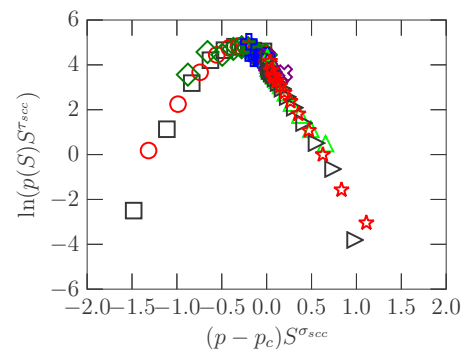


FIG. 8. Scaling behavior of the SCC size distribution  $p(S)$  for a square lattice with  $L = 4096$ , under the second parametrization. The results are for  $p = p_c + \delta$  with  $\delta = -0.01$  (black squares),  $\delta = -0.005$  (red circles),  $\delta = -0.0025$  (green diamonds),  $\delta = -0.00075$  (blue cross),  $\delta = 0.00075$  (violet  $\times$ ),  $\delta = 0.0025$  (lime up-triangles),  $\delta = 0.005$  (black right triangles), and  $\delta = 0.01$  (red stars).

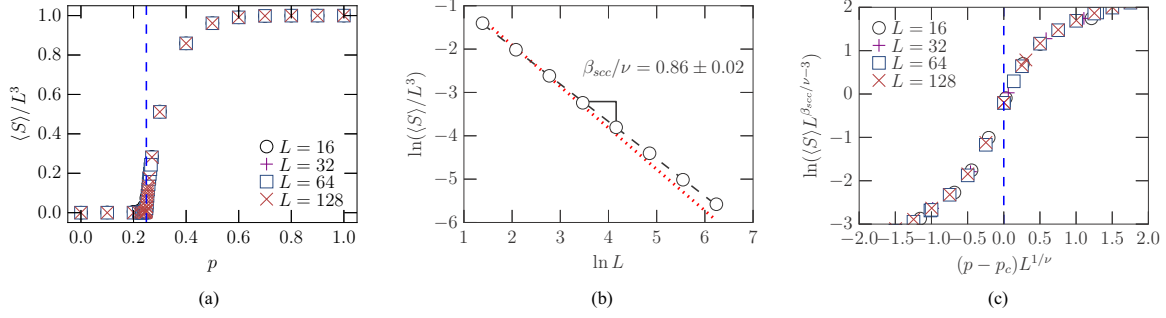


FIG. 9. These results correspond to a cubic lattice where each possible directed bond is occupied with probability  $p$ , with opposite bonds between the same pair of sites being present with probability  $p^2$ , as parametrized in Eq. (13). (a) The order parameter for percolation of isotropically directed bonds, corresponding to the fraction occupied by the largest SCC, the fraction occupied by the largest cluster decays as a power law, yielding the exponent  $\beta_{\text{SCC}}/\nu$ . The red dotted line corresponds to the form  $L^{-2\beta/\nu}$ , with  $\beta = 0.418$  and  $\nu = 0.876$  being the exponents for standard percolation in three dimensions. Given the error bar of the points and the possibility of finite-size deviations, our results allow for the possibility that in three dimensions,  $\beta_{\text{SCC}} = 2\beta$ . (c) Using the value obtained for  $\beta_{\text{SCC}}/\nu = 0.87$ , and assuming that the exponent  $\nu = 0.876$  as in standard percolation, we can collapse all the curves near the critical point.

other hand, Fig. 8 shows rescaled plots of  $p(S)$  for a triangular lattice with  $L = 1000$ , exhibiting good data collapse based on Eq. (15) with  $\tau_{\text{SCC}} = 2.11$  and  $\sigma_{\text{SCC}} = 0.414$ , in agreement with the scaling relation  $\sigma_{\text{SCC}} = 1/(\beta_{\text{SCC}} + \gamma_{\text{SCC}})$ .

Finally, we have also performed simulations on a cubic lattice under the first parametrization, Eq. (13). We simulated lattices with linear size going from  $L = 16$  to 128, taking averages over a number of samples going from 9600 ( $L = 16$ ) to 1000 ( $L = 128$ ). Figure 9 shows results concerning the order parameter, while Fig. 10 shows results concerning the second moment of the distribution of sizes of SCCs. As in the case of two dimensions, the critical point has the same value as for standard percolation,  $p_c = 0.2488$  [30,31]. At the critical point, both quantities scale as power laws, yielding the exponents  $\beta_{\text{SCC}}/\nu$  and  $\gamma_{\text{SCC}}/\nu$ . Assuming that the exponent  $\nu$  is the same as in standard percolation,  $\nu = 0.876$  [32,33], we have  $\beta_{\text{SCC}} = 0.76(1)$  and  $\gamma_{\text{SCC}} = 3.6(1)$ . As we show in Figs. 9 and 10, the curves for different system sizes can be collapsed using these values for the exponents. Figure 11 shows the distribution of sizes of SCCs for cubic lattices with  $L = 128$ . The value obtained for the Fisher exponent  $\tau_{\text{SCC}} = 2.40 \pm 0.01$  is, within error bars, consistent with the hyperscaling relation  $\tau_{\text{SCC}} = 1 + 3/d_{\text{SCC}}$ , with  $d_{\text{SCC}} = 3 - \beta_{\text{SCC}}/\nu \approx 2.13 \pm 0.01$ .

## V. DISCUSSION

We investigated the percolation of isotropically directed bonds, and we presented a conjectured expression for the location of the percolation threshold, which we showed to be exact for the square, triangular, and honeycomb lattices.

We have also performed extensive computer simulations and investigated the percolation properties of the strongly connected components (SCC), the out-components (OUT), and the in-components (IN). Contrary to what happens in directed scale-free networks [17], on the regular lattices considered in this paper the percolation threshold is the same for SCCs, OUTs, and INs. This is related to the fact that, once we are slightly above  $p_c$ , there is an infinite number of paths (in the thermodynamic limit) connecting the opposite sides of the lattice. We also obtain an apparently universal order-parameter exponent for the SCCs that is larger (or, equivalently, a fractal dimension which is smaller) than the one for both the OUTs and the INs. Moreover, the exponents obtained for the giant out-components are the same as those obtained for standard percolation [15]. This is in agreement with an approximate real-space renormalization-group prediction [9] that the order-parameter exponents are different for clusters that can be traversed only in one direction and for clusters

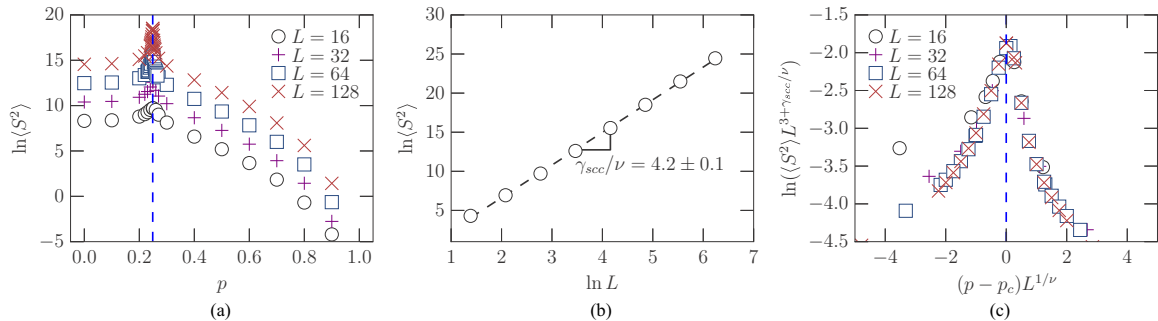


FIG. 10. These results correspond to a cubic lattice where each possible directed bond is occupied with probability  $p$ , with opposite bonds between the same pair of sites being present with probability  $p^2$ , as parametrized in Eq. (13). (a) The second moment of the distribution of sizes of SCCs, excluding the largest SCC. (b) At the critical point, the second moment grows as a power law, yielding the exponent  $\gamma_{\text{SCC}}/\nu$ . (c) Using the value obtained for  $\gamma_{\text{SCC}}/\nu$ , and assuming  $\nu = 0.876$  as in standard percolation, we can collapse all the curves near the critical point.

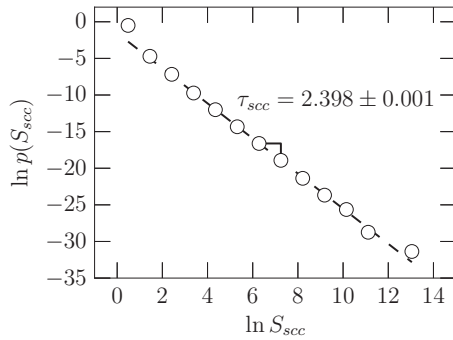


FIG. 11. Scaling behavior of the SCC size distribution  $p(S)$  for a cubic lattice with  $L = 128$ , under the second parametrization.

that can be traversed in both directions. Also, simulations in a cubic lattice allowed us to confirm that the critical point for this case also coincides with that of standard percolation. Finite-size scaling for this case shows that the exponent  $\nu$  is the same as that of standard percolation, while the exponents  $\beta_{\text{scc}}$  and  $\gamma_{\text{scc}}$  for the giant strongly connected component in percolation of isotropically directed bonds differ from those of standard percolation.

Note that the value of the order-parameter exponent obtained for the SCCs from Figs. 4(b) and 5(b) is also distinct from the value of the GOUT order-parameter exponent obtained in Refs. [12,13] as a function of the anisotropy introduced by allowing a preferred direction. In that case, the exponent is simply given by the product of a crossover exponent and the usual GOUT exponent of standard percolation.

The correlation function gives the probability that two sites separated by a distance  $r$  belong to the same cluster and, at the critical transition, decay for large distances  $r$  as  $g(r) \sim r^{-2\beta/\nu}$  [34,35]. In the case of percolation of directed bonds, different correlation functions can be defined. Here we define  $g_{\text{out}}(r)$  as the probability that a given node is in the out-component of another node separated by a distance  $r$ . Alternatively, we define  $g_{\text{scc}}(r)$  as the probability that two sites separated by a distance  $r$  belong to the same SCC. Assuming that

finding a path in one direction or the other are uncorrelated events, we have  $g_{\text{scc}}(r) = g_{\text{out}}(r) \times g_{\text{in}}(r)$ . Since the in (out) components are in the same universality class as standard percolation, we have that, considering uncorrelated events, the value of  $\beta_{\text{scc}}$  should be twice that for standard percolation. If in fact these events are correlated, one could expect  $\beta_{\text{scc}}/2$  to be smaller than the exponent  $\beta$  of standard percolation. In standard percolation, a cutting bond [36] is a bond that if removed results in the loss of connection in a cluster. In our extension, a directed bond can be a cutting bond in each direction or possible in both directions; we call this latter case a double cutting bond. The presence of double cutting bonds should lead to correlations between the connectivity events in the opposite directions. Note that the same event (including or removing this cutting bond) would determine the presence or not of a path from one side to the other in both directions. In standard percolation, the density of cutting bonds decays as  $L^{1/\nu-d}$  [36]. Considering that being a cutting bond in each direction are independent events, the density of these double cutting bonds should be the square of the density of cutting bonds in standard percolation  $L^{2/\nu-2d}$ . Since this density decreases faster than  $L^{-d}$ , the number of such double cutting bonds should be zero in large enough lattice sizes, indicating that no correlation should be observed. In the case of two dimensions, this relation is true within the error bars,  $\beta_{\text{scc}} = 0.27 \pm 0.01 \approx 2 \times 5/36 = 0.2777$ . In the case of three dimensions, the obtained value for  $\beta_{\text{scc}} = 0.76 \pm 0.08$  is smaller than expected, as the value of standard percolation is  $\beta = 0.418 \pm 0.001$  [32]. However, this deviation is still within the error bars and may also arise from finite-size effects.

#### ACKNOWLEDGMENTS

We thank the Brazilian agencies CNPq, CAPES, FUN-CAP, NAP-FCx, the National Institute of Science and Technology for Complex Fluids (INCT-FCx), and the National Institute of Science and Technology for Complex Systems (INCT-SC) in Brazil for financial support.

- 
- [1] S. R. Broadbent and J. M. Hammersley, *Math. Proc. Cambridge Philos. Soc.* **53**, 629 (1957).
  - [2] D. Stauffer and A. Aharony, *Introduction To Percolation Theory* (Taylor & Francis, London, 1994).
  - [3] J. Marro and R. Dickman, *Nonequilibrium Phase Transitions in Lattice Models* (Cambridge University Press, Cambridge, 2005).
  - [4] C. Fortuin and P. Kasteleyn, *Physica* **57**, 536 (1972).
  - [5] F. W. S. Lima, *J. Phys.: Conf. Ser.* **246**, 012033 (2010).
  - [6] Y.-Y. Liu and A.-L. Barabási, *Rev. Mod. Phys.* **88**, 035006 (2016).
  - [7] M. Santolini and A.-L. Barabási, *Proc. Natl. Acad. Sci. USA* **27**, E6375 (2018).
  - [8] D. Li, B. Fu, Y. Wang, G. Lu, Y. Berezin, H. E. Stanley, and S. Havlin, *Proc. Natl. Acad. Sci. USA* **112**, 669 (2015).
  - [9] S. Redner, *J. Phys. A* **14**, L349 (1981).
  - [10] S. Redner, *Phys. Rev. B* **25**, 3242 (1982).
  - [11] S. Redner, *Phys. Rev. B* **25**, 5646 (1982).
  - [12] N. Inui, H. Kakuno, A. Yu. Tretyakov, G. Komatsu, and K. Kameoka, *Phys. Rev. E* **59**, 6513 (1999).
  - [13] H.-K. Janssen and O. Stenull, *Phys. Rev. E* **62**, 3173 (2000).
  - [14] O. Stenull and H.-K. Janssen, *Phys. Rev. E* **64**, 016135 (2001).
  - [15] Z. Zhou, J. Yang, R. M. Ziff, and Y. Deng, *Phys. Rev. E* **86**, 021102 (2012).
  - [16] S. N. Dorogovtsev, J. F. F. Mendes, and A. N. Samukhin, *Phys. Rev. E* **64**, 025101 (2001).
  - [17] N. Schwartz, R. Cohen, D. ben Avraham, A.-L. Barabási, and S. Havlin, *Phys. Rev. E* **66**, 015104 (2002).
  - [18] M. Bogaña and M. A. Serrano, *Phys. Rev. E* **72**, 016106 (2005).
  - [19] E. Kenah and J. M. Robins, *Phys. Rev. E* **76**, 036113 (2007).
  - [20] M. Ángeles Serrano and P. De Los Rios, *Phys. Rev. E* **76**, 056121 (2007).
  - [21] M. Franceschet, *J. Am. Soc. Inform. Sci. Technol.* **63**, 837 (2012).

- [22] Y.-X. Zhu, X.-G. Zhang, G.-Q. Sun, M. Tang, T. Zhou, and Z.-K. Zhang, *PLoS ONE* **9**, e103007 (2014).
- [23] R. E. Tarjan, *SIAM J. Comput.* **1**, 146 (1972).
- [24] P. L. Leath, *Phys. Rev. B* **14**, 5046 (1976).
- [25] Z. Alexandrowicz, *Phys. Lett. A* **80**, 284 (1980).
- [26] S. N. Dorogovtsev, *J. Phys. C* **15**, L889 (1982).
- [27] M. F. Sykes and J. W. Essam, *J. Math. Phys.* **5**, 1117 (1964).
- [28] T. P. Peixoto *figshare* (2014), doi:10.6084/m9.figshare.1164194.
- [29] A. Stauffer and D. Aharony, *Introduction to Percolation Theory* (CRC Press, Boca Raton, FL, 1994).
- [30] J. Wang, Z. Zhou, W. Zhang, T. M. Garoni, and Y. Deng, *Phys. Rev. E* **87**, 052107 (2013).
- [31] C. D. Lorenz and R. M. Ziff, *Phys. Rev. E* **57**, 230 (1998).
- [32] H. G. Ballesteros, L. A. Fernandez, V. Martin-Mayor, A. M. Sodupe, G. Parisi, and J. J. Ruiz-Lorenzo, *J. Phys. A* **32**, 1 (1999).
- [33] H. Hu, H. W. J. Blöte, R. M. Ziff, and Y. Deng, *Phys. Rev. E* **90**, 042106 (2014).
- [34] M. E. Fisher, *Rev. Mod. Phys.* **46**, 597 (1974).
- [35] N. R. M. Kim Christensen, *Complexity and Criticality*, Imperial College Press Advanced Physics Texts Vol. 1 (Imperial College Press, London, 2005).
- [36] A. Coniglio, *J. Phys. A* **15**, 3829 (1982).